Article:
Yang, Jiannan orcid.org/0000-0001-8323-7406, Clot, Arnau and Langley, Robin S. (2022) Combined sensitivity analysis for multiple failure modes. Computer Methods in Applied Mechanics and Engineering. 115030. ISSN: 0045-7825

https://doi.org/10.1016/j.cma.2022.115030

Available online at www.sciencedirect.com
ScienceDirect
Comput. Methods Appl. Mech. Engrg. 395 (2022) 115030
Computer methods in applied mechanics and engineering
www.elsevier.com/locate/cma

Combined sensitivity analysis for multiple failure modes

Jiannan Yang*, Arnau Clot[1], Robin S. Langley

Department of Engineering, University of Cambridge, Trumpington Street, Cambridge CB2 1PZ, UK

Received 23 October 2021; received in revised form 29 March 2022; accepted 15 April 2022
Available online 10 May 2022

Abstract

Sensitivity analysis identifies the influential parameters and it is a key step in the design process. Focusing on reliability based design, the probability of a failure mode and its sensitivity to input uncertainties are obtained in a single Monte Carlo simulation using the Likelihood Ratio method. For correlated multiple failure modes, a sensitivity matrix is proposed. The dominant singular vectors of the sensitivity matrix are found to indicate the most important parameters for combined sensitivity of multiple failure modes. Therefore, the sensitivity matrix can guide resources allocation so that most uncertainties can be reduced for system reliabilities.

Keywords: Correlated failure modes; Sensitivity to distribution parameters; System reliability; Sensitivity matrix; Likelihood ratio method; Marine riser

1. Introduction

Despite the ubiquitous presence of uncertainties in real engineering systems, a common practice in engineering design is to assume nominal values for the uncertain parameters and employ safety factors to mitigate the potential risk. This often results in much conserved designs. When considered explicitly in the design process, uncertainties are characterised by mathematical representations based on theories such as probability theory, possibility theory and interval analysis and a detailed comparison is given in [1]. Irrespective of the mathematical representations, an explicit consideration of uncertainties often leads to two main types of design [2,3]: (1) robust design, in which measures are sought to gauge the robustness of the design output; (2) reliability-based design, in which the design is assessed against a given threshold. When a probabilistic approach is used, reliability-based design leads to assessment of the expected failure probabilities against the design threshold. Because it is more computational demanding to quantify uncertainties explicitly, much research has focused on searching for efficient numerical methods; summaries can be found in [4] for reliability-based design and in [5] for robust design. Once uncertainties are quantified in the design, it is desirable to conduct sensitivity analysis to understand the relative importance of the different sources of uncertainties [6]. Sensitivity analysis helps designers to focus resources of reducing dominant uncertainties and to fix less sensitive uncertain parameters to simplify the numerical models. More importantly, it improves our understanding of the relationship between input parameters and functional performances of the design.

* Corresponding author.
E-mail address: jy419@cam.ac.uk (J. Yang).
[1] Present address: Serra Húnter Fellow, Universitat Politècnica de Catalunya (UPC). c/ Colom, 11, 08222 Terrassa (Barcelona), Spain.

https://doi.org/10.1016/j.cma.2022.115030

In the context of structural engineering design, the input parameters are often classified into design variables which are deterministic, and random variables which contain all uncertainties involved in the design [2]. On one hand, when the target is to utilise the sensitivity information to find the optimal design point using line searches, it is often necessary to obtain the gradients of the objective function with respect to the design variables [7,8]. The gradients with respect to the design variables can be obtained using polynomial chaos method because a functional relationship between the uncertain response and each of its input variables is represented as polynomial expansions [9]. However, for reliability-based design, application of the polynomial chaos method is more difficult because the failure region is often unknown. In [10], an indicator function is introduced to transform the failure region to the full random space and a smooth approximation is adopted to compute the gradients. When the Monte Carlo methods are used, the numerical efforts involved in the calculation of the failure probabilities can be prohibitive [3]. As a result, the gradients of the failure probability to deterministic variables are often estimated by approximation of the performance functions [11,12]. On the other hand, if the purpose of sensitivity analysis is to reduce design uncertainties, the gradient of interest is often with respect to the distribution parameters of the uncertain variables. This is because normally partial derivative with respect to a random variable does not have mathematical support, unless it is the realisations of the random variable that is of interest [10]. An extended polynomial chaos formalism has been applied for evaluating the sensitivities of output distribution functions to input distribution parameters in [13], where the failure probabilities are treated as random variables themselves for applications to reliability sensitivity. One of the approaches that is widely adopted in this category is the Likelihood Ratio (LR) method [14], also known as score function method [15], where sensitivities of the response function are computed with respect to the distribution parameters of the random variables. Although a well-developed gradient estimation method, especially for Monte Carlo based stochastic optimisations, application of LR method in reliability sensitivity analysis has only become popular recently, see [15–18].

Despite various methods exist for sensitivity analysis, many of them are derivative based [6]. In its simplest form, the sensitivity is obtained using the partial derivatives of the model with respect to its input factors. One of the main drawbacks is that, although it is more informative to explore the entire space with random inputs, the partial derivatives tend to only provide local information. The application of the derivative-based sensitivity analysis is also limited in cases where it is difficult to compute the derivatives directly. For example, partial derivatives are often approximated using finite difference methods for black box models.

In this paper, we conduct sensitivity analysis to identify the most influential uncertain variables in the design. As pointed out in a recent investigation of design formulations in the presence of uncertainties [3], different strategies exist for robust design while a consensus is reached to measure failure probabilities for reliability-based design. Therefore, although the proposed sensitivity metric is applicable to a wide range of performance measures, in this paper we will focus on sensitivities of failure probabilities for reliability-based design. We propose a new metric for combined sensitivity of engineering systems that have multiple failure modes. Taking advantage of its rigorous definition and familiarity to practitioners, the sensitivity analysis in this paper is based on partial derivatives. We examine the sensitivity with respect to, not directly the random input variables, but their distribution parameters (e.g. mean or standard deviation). Note that as the adopted method is based on partial derivatives, it is a local sensitivity method with respect to the distribution parameters of the random input variables. Once the gradient vectors of each individual failure modes are obtained, they are normalised and assembled as the sensitivity matrix. The combined sensitivity of multiple correlated failure modes is then studied via singular value decomposition of the sensitivity matrix. The gradients of the failure probabilities in this study are obtained via the Likelihood Ratio (LR) method [14]. When used in combination with Monte Carlo sampling, the LR method is efficient because only a single simulation run is required to obtain the failure probability and its gradient to distribution parameters. It is noted in passing that the proposed sensitivity analysis is applicable for both epistemic and aleatory uncertainties, but further design decisions are dependent on the uncertainty type, i.e. reducible or irreducible, of the identified influential parameters.

In what follows, the sensitivity matrix for combined sensitivity of multiple correlated failure modes is proposed in Section 2. In the same section, the key components to compute failure probability sensitivities and the corresponding numerical steps are introduced (Fig. 1 and Algorithm 1). Numerical results of a case study from sensitivity analysis of an offshore marine riser using the proposed method are given in Section 3, where three failure modes and system failures with different configurations of the individual modes are analysed. A convergence and validation analysis is presented in Appendix C for the numerical case considered. In Section 4, the role of the singular vectors of the sensitivity matrix is discussed and the normalised sensitivity is critically reviewed for practical implementations. Concluding remarks are given in Section 5.

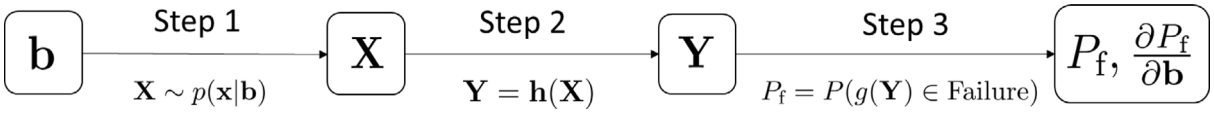

Fig. 1. Numerical steps for analysis of the failure probability and its gradient to **b**. **X** is a vector of random variables and **b** is a vector of corresponding distribution parameters (e.g. mean or standard deviation). **Y** is the design quantities of interest output from a numerical model **h**, where **h** can be black box models. $P_\mathrm{f}(\mathbf{b}, z)$ is the failure probability and it is a function of the parameters **b** and the failure threshold z. More details of the steps are given in Section 2.5.

2. Method

2.1. Failure probabilities

Reliability analysis concerns the probability of failure P_f of the object under design, i.e., the probability that a certain quantity is over/below a given threshold z. An unconditional probability of failure can be expressed as

$$P_\mathrm{f}(\mathbf{b}, z) = \int P_\mathrm{f}(\mathbf{h}(\mathbf{x}), \mathbf{x}, z)\, p(\mathbf{x}|\mathbf{b}) \mathrm{d}\mathbf{x} \tag{1}$$

where **x** is a vector of the realisations corresponding to random variable vector **X** and **b** is a vector of corresponding distribution parameters. For example, when X is a Gaussian random variable, the corresponding distribution parameters are the mean and stand deviation, i.e. $\mathbf{b} = (\mu, \sigma)$. $P_\mathrm{f}(\mathbf{h}(\mathbf{x}), \mathbf{x}, z)$ is the conditional probability of failure that would depend on the realisations of the random variables and the design criteria z. In addition, the conditional failure probability is in general a function of the quantity of interest $\mathbf{Y} = \mathbf{h}(\mathbf{x})$ as shown in Fig. 1. For example, in the fatigue failure case described in Section 3, fatigue damage $g(\mathbf{Y})$ is a function of the random stress response **Y** computed from the dynamic model of an offshore marine riser and failure occurs when the damage received by the structure exceeds its capacity during its design life. In Eq. (1), $p(\mathbf{x}|\mathbf{b})$ is the joint probability density function (PDF) of **x**. It is assumed in this paper that the components of **x** are independent, that is:

$$p(\mathbf{x}|\mathbf{b}) = \prod_i p_i\left(x_i \,|b_{i,1}, \ldots\right) \tag{2}$$

where p_i is the PDF considered for the random variable x_i. To simplify the notation, when the context is clear, subscript i will be dropped for **b** vector in subsequent sections, and P_f is used to indicate the unconditional failure probability $P_\mathrm{f}(\mathbf{b}, z)$ for a given threshold z.

2.2. Sensitivity of failure probabilities

The purpose of the sensitivity analysis in this work is to identify the most important uncertain parameters or factors in the design. The designer can then make informed decisions to prioritise the resources for further analyses or measurements. With this objective, we look at the perturbed effect on the (unconditional) failure probability using the first order Taylor expansion from the nominal values of **b**

$$\begin{aligned} P_\mathrm{f}^{(k)}(\mathbf{b} + \Delta\mathbf{b}) &= P_\mathrm{f}^{(k)}(\mathbf{b}) + \Delta P_\mathrm{f}^{(k)} \\ &\approx P_\mathrm{f}^{(k)}(\mathbf{b}) + \frac{\partial P_\mathrm{f}^{(k)}}{\partial \mathbf{b}} \Delta\mathbf{b} \end{aligned} \tag{3}$$

where $P_\mathrm{f}^{(k)}$ is the failure probability for a single failure mode (the superscript k indicates kth failure mode in system analysis to be introduced in Section 2.3). The partial derivative vector, $\partial P_\mathrm{f}^{(k)}/\partial\mathbf{b}$, then provides the relative effect on the perturbations of the failure probability for an infinitesimal change of **b**. However, these raw partial derivatives are not directly comparable when the parameters are of different units. One approach to overcome this issue is to normalise the raw derivative as:

$$r_{jk} = \frac{\partial P_\mathrm{f}^{(k)}}{\partial b_j} \frac{b_j}{P_\mathrm{f}^{(k)}} \tag{4}$$

where the normalised derivative r is often called proportional sensitivity or elasticity [19] and it measures the percentage change on P_f resulting from a fraction change of b. Therefore, r can be used to compare the relative sensitivities of parameters of different physical units because it is dimensionless. In addition, it is straightforward to show that r is invariant under rescaling of the variables in the equation [20]. Further discussion is given in Section 4.3 for practical design implementation of the proportional sensitivity metric.

2.3. Combined sensitivity for multiple failure modes

2.3.1. System failure sensitivity for simple systems

Engineering systems often have multiple failure modes. Either it could be a single component subject to different failure mechanisms or the system might consist of multiple components. In the system level, it is often simplest to consider the multiple failure modes in either series or parallel configurations [21]. For simplicity, let us consider the failure modes are independent (note that independence is only assumed in this section for illustration of the motivation using simple systems and full analysis are conducted for the case study in Section 3).

If multiple failure modes are considered to be in series, i.e. the system fails if any one of the failure mode occurs, the system failure probability is (assuming small failure probabilities):

$$P_\mathrm{f} = \sum_k P_\mathrm{f}^{(k)} \tag{5}$$

Then it is easy to show that the normalised system failure sensitivity is (with respect to b_j):

$$\frac{\partial P_\mathrm{f}}{\partial b_j}\frac{b_j}{P_\mathrm{f}} = \sum_k \frac{\partial P_\mathrm{f}^{(k)}}{\partial b_j}\frac{b_j}{P_\mathrm{f}} = \frac{1}{P_\mathrm{f}}\sum_k \frac{\partial P_\mathrm{f}^{(k)}}{\partial b_j}\frac{b_j}{P_\mathrm{f}^{(k)}}P_\mathrm{f}^{(k)} \tag{6}$$

Denoting the normalised system sensitivity with respect to b_j as s_j, we can rewrite Eq. (6) more compactly as:

$$s_j = \frac{1}{P_\mathrm{f}}\sum_k r_{jk}P_\mathrm{f}^{(k)} \tag{7}$$

If the failure modes are considered to be in parallel, i.e. the system only fails if all failure modes occur, the system failure probability is:

$$P_\mathrm{f} = \prod_k P_\mathrm{f}^{(k)} \tag{8}$$

Taking natural logarithm of both sides of Eq. (8), and differentiate with respect to b_j, we get

$$\frac{\partial \ln P_\mathrm{f}}{\partial b_j} = \frac{1}{P_\mathrm{f}}\frac{\partial P_\mathrm{f}}{\partial b_j} = \sum_k \frac{1}{P_\mathrm{f}^{(k)}}\frac{\partial P_\mathrm{f}^{(k)}}{\partial b_j} \tag{9}$$

Multiply both sides by b_j in Eq. (9), the normalised system failure sensitivity is then:

$$s_j = \sum_k r_{jk} \tag{10}$$

It can be seen from Eqs. (7) and (10) that for simple failure configurations (serial or parallel), the system failure sensitivity is a linear combination of sensitivities from independent individual modes. However, general systems have more complicated configurations and the individual failure modes are most likely to be correlated for the same system. To overcome this issue, we propose a sensitivity matrix $\mathbf{R}$ to look at the combined sensitivity of general systems in the next section.

2.3.2. Sensitivity matrix $\mathbf{R}$ for general systems

The observation from simple cases in Section 2.3.1 prompts the idea that information about the system sensitivity can be obtained by looking into linear combinations of the sensitivity vectors from individual failure modes. In other

words, we can assemble a sensitivity matrix $\mathbf{R}$, with the individual sensitivity vectors as the columns:

$$\mathbf{R} = \begin{bmatrix} r_{11} & \cdots & r_{1k} & \cdots & r_{1n} \\ \vdots & \ddots & & & \\ r_{j1} & & r_{jk} & & \\ \vdots & & & \ddots & \\ r_{m1} & & & & r_{mn} \end{bmatrix} \tag{11}$$

where the size of $\mathbf{R}$ is m by n, with n failure modes corresponding to the columns and the rows for m parameters. From the observations in Section 2.3.1, the system sensitivity information is a linear combinations of independent vectors in the column space of matrix $\mathbf{R}$. However, the individual sensitivity vectors, or the columns of matrix $\mathbf{R}$, are in general not independent. To find a good basis for the column space of matrix $\mathbf{R}$, we can use its left singular vectors that have nonzero singular values (right singular vectors correspond to row space of the matrix). With the orthogonal singular vectors, the combinations of multiple failure modes can be decomposed into independent, non-interacting elements.

The above reasoning to form the sensitivity matrix $\mathbf{R}$ is based on a heuristic basis. In Appendix A, the method of Lagrange Multiplier is used to solve a constrained optimisation problem where the combined perturbation of multiple failure modes are maximised. It is demonstrated analytically in Appendix A that the singular vectors of $\mathbf{R}$ not just decouple the combined effect from multiple failure sensitivities, the vector that perturbs the combined failure probability the most, are the singular vectors with largest singular values. Therefore, the dominant singular vectors can guide designers to focus the design resources because they represent the directions of maximum change of the combined failure probability. This is demonstrated numerically from the case study of the marine riser in Section 3.4. As to be shown in Fig. 6(a) for different configuration of multiple failure modes, it is the first singular vector of matrix $\mathbf{R}$ that dominates the projection of system failure sensitivities.

In cases where the system failure configurations are known, the system failure probability and its sensitivity can also be computed using Eqs. (14) and (15), where in this case the joint probability from multiple modes are used. In this case, as discussed in Section 4.2, the singular vectors of $\mathbf{R}$ still provide useful information about the relative weighting of individual modes to help target the resources for system design improvement.

2.4. Likelihood ratio method

Sensitivity analysis for individual failure modes needs to be conducted to get the sensitivity matrix $\mathbf{R}$. The largest effort in evaluation of the proportional sensitivity in Eq. (4) is the determination of the partial derivatives. In a standard setting, especially for black box functions, the model has to be evaluated twice and take the approximation of the derivative with finite difference method. This is time consuming for complicated simulations with Monte Carlo method. In this paper, we use the Likelihood Ratio (LR) method to overcome this issue. Likelihood Ratio (aka score function) method obtains gradient estimation of a performance measure with respect to (w.r.t.) continuous parameters in a single simulation run [14], and it is independent of the dimension d of the parameters of interest [18]. Applying the LR method to Eq. (1), the partial derivative of the failure probability to the distribution parameter $\mathbf{b}$ can be computed as:

$$\begin{aligned} \frac{\partial P_{\mathrm{f}}(\mathbf{b})}{\partial \mathbf{b}} &= \int P_{\mathrm{f}}(\mathbf{x}) \frac{\partial p(\mathbf{x}|\mathbf{b})}{\partial \mathbf{b}} \mathrm{d}\mathbf{x} \\ &= \int P_{\mathrm{f}}(\mathbf{x}) \frac{\partial \ln p(\mathbf{x}|\mathbf{b})}{\partial \mathbf{b}} p(\mathbf{x}|\mathbf{b}) \mathrm{d}\mathbf{x} \end{aligned} \tag{12}$$

where the jth term of the vector $\partial P_{\mathrm{f}}/\partial \mathbf{b}$ is the partial derivative $\partial P_{\mathrm{f}}/\partial b_j$ ($j = 1, \ldots, d$). The derivation above uses the fact that the conditional probability of failure $P_{\mathrm{f}}(\mathbf{x})$ in the integrand of Eq. (12) is independent of the parameters $\mathbf{b}$ with a given $\mathbf{x}$, i.e. $\mathbf{b} \rightarrow \mathbf{x} \rightarrow P_{\mathrm{f}}(\mathbf{x})$ form a Markov chain. In addition, the technique used in importance sampling has been adopted here by multiplying the ratio of the PDF $p(\mathbf{x}|\mathbf{b})$ to itself, i.e. ratio of one.

The main advantage of expressing the sensitivities as above is that both the probability of failure calculation and its sensitivities can be approximated using Monte Carlo integration, which means that almost all the computational effort of the calculation is done in obtaining $P_{\mathrm{f}}(\mathbf{x})$ for each set of samples. For many commonly used distributions,

analytical closed-form expressions can be obtained for the additional terms involving the partial derivatives w.r.t. a distribution parameter. For example, for Gaussian distribution:

$$\frac{\partial \ln p(x|\mu,\sigma)}{\partial \mu} = \frac{x-\mu}{\sigma}; \quad \frac{\partial \ln p(x|\mu,\sigma)}{\partial \sigma} = \frac{(x-\mu)^2-\sigma^2}{\sigma^3} \tag{13}$$

and the LR expressions for a list of commonly used distributions can be found in [16].

To validate the proposed sensitivity estimation using the Likelihood Ratio method, a comparison between the exact and approximate perturbation of the probability of failure is presented in Appendix C. The exact method calculates the change of the failure probability by $\Delta P_{\mathrm{f}}^{j} = P_{\mathrm{f}}\left(\mathbf{b}+\Delta b_j\right) - P_{\mathrm{f}}(\mathbf{b})$ with direct perturbation of the input parameters. In comparison, the approximation calculates the perturbation via 1st order perturbation $\Delta P_{\mathrm{f}}^{j} = \Delta b_j \partial P_{\mathrm{f}}/\partial b_j$. The exact results are based on perturbing one parameter at a time, and the computational cost increases as the number of parameters increases which will inevitably become prohibitive as the number of parameters gets larger. On the other hand, the proposed method using the Likelihood Ratio method just requires a single run to get the sensitivities to all parameters of interest.

2.5. Monte Carlo implementation

Numerical steps to calculate failure probabilities and the corresponding sensitivities to the assumed distribution parameters are summarised in Fig. 1 and is compiled below in Algorithm 1. These results are obtained computing the integrals in Eq. (1) for P_{f} and Eq. (12) for $\partial P_{\mathrm{f}}/\partial \mathbf{b}$ with a Monte Carlo integration scheme. The procedure can be divided into the following steps. First define PDFs $p(\mathbf{x}|\mathbf{b})$ for the input uncertain variables, draw N_s sets of samples for the random variable vector $\mathbf{X} \sim p(\mathbf{x}|\mathbf{b})$. Then evaluate the function $\mathbf{Y} = \mathbf{h}(\mathbf{X})$ N_{s} times for the quantities of interest, e.g. random bending stress response. The conditional failure probability is in general a function of the quantity of interest $\mathbf{Y} = \mathbf{h}(\mathbf{x})$, for example, fatigue damage $g(\mathbf{Y})$ is a function of the random stress response $\mathbf{Y}$ computed from the dynamic model of an offshore marine riser and failure occurs when the damage received by the structure exceeds its capacity during its design life. Compute the conditional probability of failure for each sample of the set of parameters: $P_{\mathrm{f}}(\mathbf{x}_n)$. The unconditional probability of failure and its sensitivity to a distribution parameter b_{j} can then be obtained numerically using the Monte Carlo methods below:

$$P_{\mathrm{f}} \approx \frac{1}{N_{\mathrm{s}}} \sum_n P_{\mathrm{f}}(\mathbf{x}_n) \tag{14}$$

$$\frac{\partial P_{\mathrm{f}}}{\partial b_j} \approx \frac{1}{N_{\mathrm{s}}} \sum_n \left[P_{\mathrm{f}}(\mathbf{x}_n) \frac{\partial \ln p(\mathbf{x}_n|\mathbf{b})}{\partial b_j} \right] \tag{15}$$

where n refers to the nth set of sample. The expressions in Eq. (13) can be used for the derivative terms.

Algorithm 1: Monte Carlo implementation for sensitivity estimation
1. Define probability density function (PDF) for the input uncertain variables $p(\mathbf{x}\|\mathbf{b})$
2. Derive the partial derivatives expression $\partial \ln p(\mathbf{x}\|\mathbf{b})/\partial b_j$ for each distribution parameter b_j. This is often available in closed-form analytically, e.g. see Eq (13) for Gaussian distribution
3. **for** $n \leftarrow 1$ to N_s
4. draw one set of sample $\mathbf{x}_n$ from $p(\mathbf{x}\|\mathbf{b})$
5. evaluate the black box function $\mathbf{Y}_n = \mathbf{h}(\mathbf{x}_n)$ and/or $g(\mathbf{Y}_n)$ as shown in Figure 1
6. compute the conditional probability of failure $P_{\mathrm{f}}(\mathbf{x}_n)$ against a given threshold, e.g. $P_{\mathrm{f}} = 1$ if $\mathbf{Y}_n \geq \mathbf{z}$, or $g(\mathbf{Y}_n) \geq z$
7. substitute $\mathbf{x}_n$ into $\partial \ln p(\mathbf{x}\|\mathbf{b})/\partial b_j$ and calculate $P_{\mathrm{f}}(\mathbf{x}_n)\, \partial \ln p(\mathbf{x}_n\|\mathbf{b})/\partial b_j$
8. **end for**
9. Use the Monte Carlo estimator to evaluate unconditional failure probability and its sensitivity according to Eq (14) and (15)

Since sampling methods are used for the evaluation and the partial derivative is obtained via the Likelihood Ratio (LR) method, the function $\mathbf{h}$ can be black box models. Note that in this study, only the standard Monte Carlo method

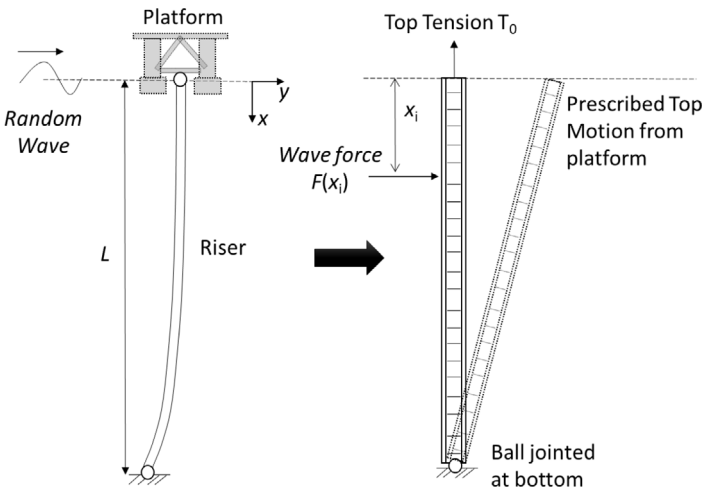

Fig. 2. Dynamic model for an offshore marine riser subject to random wave. Both ends of the riser are ball jointed and there is a prescribed top motion.

is used. This can become prohibitive when a large number of samples are evaluated. Advanced simulation methods, such as importance sampling and subset simulation, are available to mitigate this shortcoming and a survey for their application on reliability problems are available in [4]. Application of Monte Carlo methods in the framework of high performance computing environments is considered in [22].

3. Case study

The method described in Section 2 has been applied to the reliability sensitivity analysis of an offshore marine riser, as shown in Fig. 2. The riser is subject to a random wave excitation and its dynamic response is obtained using a linearised frequency domain model. The model of the marine riser used here is based on [23] and only the quantities related to this paper are briefly introduced in Appendix B. It is considered as a black-box model where only the responses of interest are required for the reliability sensitivity analysis. A convergence analysis in terms of number of Monte Carlo samples and a validation analysis for sensitivity results are presented in Appendix C using the fatigue failure mode as an example.

This example is chosen here for several reasons. First, as an illustrative example it is also of great practical significance. In the design code of offshore structures, uncertainty and sensitivity analysis are key elements [24]. Second, due to nonlinearities and random loading, there is no simple relationship between output and input. The case study therefore demonstrates the applicability of the proposed sensitivity metric for complicated black-box problems. Third, despite its complexity, the dynamic response of a marine riser has been well studied [23]. Therefore, the confidence in the numerical model is high.

3.1. List of random variables

Although there can be a large number of uncertain parameters for marine riser analysis [25], we focus on a limited subset of the model parameters to provide validation for the proposed sensitivity metric. The distribution parameters of random variables used in this example are listed in Table 1. Without loss of generality, Gaussian distributions are assumed for all the random variables, with the mean taken from their nominal values [23] and the standard deviation based on assumed coefficient of variation (CoV). The probabilistic model of the random variables for real design should be based on analysis of available data and project specific information. In case those are not available, some recommendations for fatigue analysis of a marine riser are given in [25].

Table 1
Mean and standard deviation values for the random variables.

Random variable		Mean	Standard deviation	Coefficient of variation
Morison's equation added mass coefficient	C_a [–]	1.5	0.3	0.20
Morison's equation drag coefficient	C_d [–]	1.1	0.22	0.20
Marine riser steel density	ρ [kg/m^{-3}]	7840	392	0.05
Marine riser Young's modulus	E [GPa]	200	10	0.05
Riser internal oil density	ρ_o [kg/m^{-3}]	920	92	0.10
Marine riser top tension	T_0 [kN]	4905	490.5	0.10
Material S–N curve coefficients	α [GPa]	199	19.9	0.10
	δ [–]	3	0.3	0.10

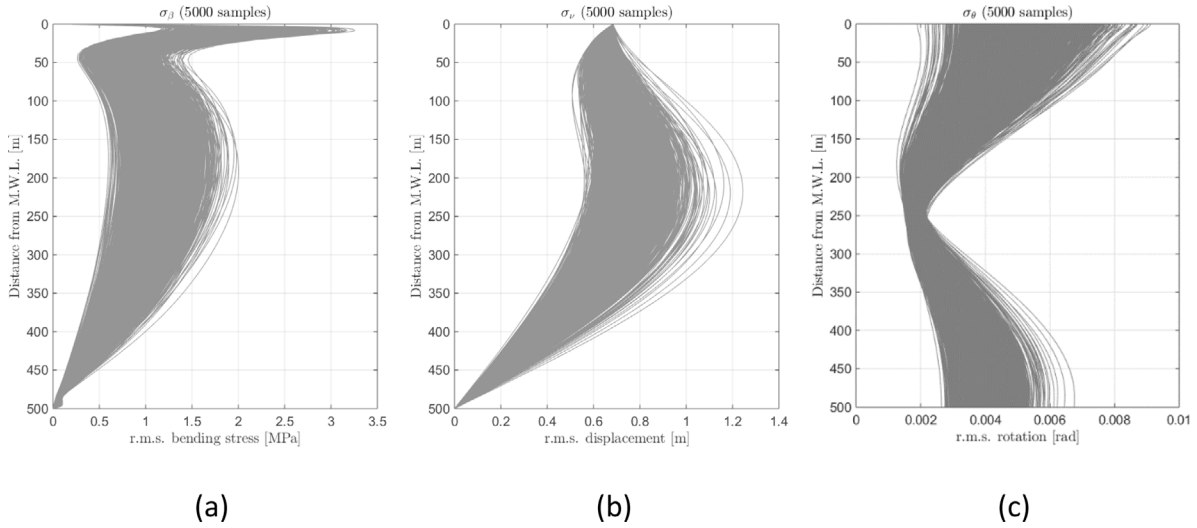

Fig. 3. Root mean square (r.m.s.) response along the riser due to random wave excitation, with the mean water level (MWL) as the origin for the coordinate. The results are from MC analysis with 5000 samples and each curve represents results from a single sample. (a) bending stress β; (b) horizontal displacement ν; (c) rotation ϑ.

3.2. Response from the black-box model

Following the procedure shown in Fig. 1 and Algorithm 1 responses form the black-box model of a marine riser are obtained from Monte Carlo (MC) analysis with 5000 samples (a convergence analysis is shown in Appendix C). The quantities of interest are the root mean square (r.m.s.) bending stress, displacement and the small rotations along the riser and they are shown in Fig. 3. It can be seen from Fig. 3 that the peak bending stress and peak rotation are located close to the mean water level, while the peak displacement is around half way down the water depth.

3.3. Failure sensitivities of individual modes

Three failure modes are analysed, fatigue failure, excessive displacement failure and excessive rotation failure. The failure probabilities and its first derivative are computed using Eqs. (14) and (15). Fatigue damage has been computed assuming a narrow band Gaussian process for the stress response and a fatigue failure is considered to occur when the damage received by the structure exceeds its capacity during its design life [25]. Failure for excessive displacement and rotation occur when the r.m.s. levels are higher than a certain percentage of the peak values (of all samples) shown in Fig. 3. For illustration purpose, example results are given with high level of failure probabilities, in the order of 0.1, for all three failure modes to maintain a low computation cost. The fatigue life is set to be 80 years and between 10% and 15% of samples would fail for excessive displacement and rotation.

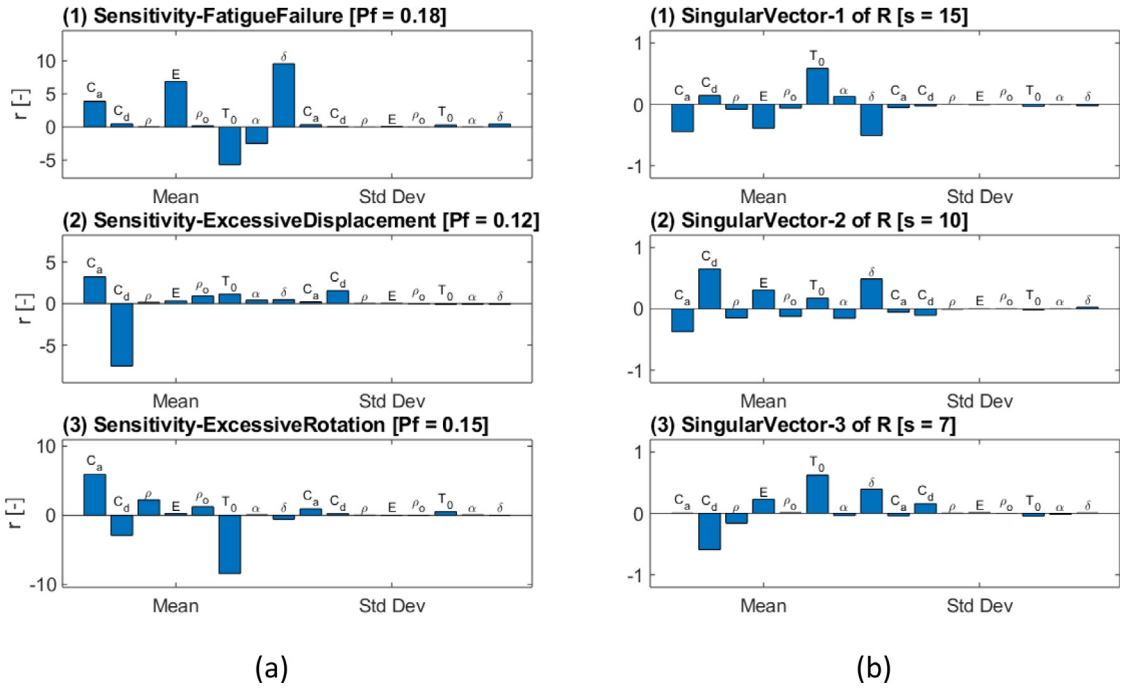

Fig. 4. (a) Proportional sensitivity r of individual failure modes with P_f indicated. (b) Singular vectors of **R** matrix with singular values s. The sensitivities are of two groups, with respect to the mean and the standard deviation (std dev). The corresponding random variables are indicated.

The proportional sensitivity r, as normalised using Eq. (4), from each failure mode are shown in Fig. 4(a). In Fig. 4(a) the sensitivities to mean and standard deviation (Std Dev) of the variables listed in Table 1 are grouped with the corresponding random variables indicated. It can be seen from Fig. 4(a-1) that fatigue failure is extremely sensitive to the S–N curve coefficient δ. This is an expected result as the total damage received by the structure depends on a factor raised to the δ power. Factors closely related to bending stress, like Young modulus E and top tension T_0, are also found to be significant for fatigue failure sensitivities. The top tension T_0 is also an important factor for the failure due to excessive rotation, as seen from Fig. 4(a-3). This is because the maximum r.m.s. rotations along the riser are located close to the water surface (Fig. 3(c)) where top tension T_0 is important. On the other hand, for failure due to excessive displacement, top tension T_0 is less important because the peak responses are dominated by dynamic resonances half way along the riser as shown in Fig. 3(b). In this case, the drag coefficient, which contributes to the damping, tends to be important as shown in Fig. 4(a-3).

The sensitivity vectors of the three failure modes form the sensitivity matrix **R** in Eq. (11). The singular vectors of the **R** matrix are shown in Fig. 4(b), with the corresponding singular values s. The singular vectors are in descending order based on their singular values.

3.4. System failure sensitivity

To look at the combined effect, the system failure probability and its sensitivity can also be computed using Eqs. (14) and (15), where in this case the joint probability from multiple modes are used (this is only applicable if the details of failure configuration is known). Note that in this case study, no assumption of independence between the different failure modes has been made. Therefore, the simplified equations in Section 2.3.1 are not applicable and the computation of the system failure probability is based on Monte Carlo simulations using Eqs. (14) and (15).

Four different cases of system failure are considered with the corresponding failure configurations listed in Table 2. The failure regions for the three individual failure modes are labelled as A for fatigue, B for excessive displacement and C for excessive rotation.

Table 2
Four different cases considered for system failure configurations.

Case no.	System failure configuration
1	$P(\mathrm{A} \cup \mathrm{B} \cup \mathrm{C})$
2	$P(\mathrm{A} \cup \mathrm{B} \cap \mathrm{C})$
3	$P(\mathrm{A} \cap \mathrm{B} \cup \mathrm{C})$
4	$P(\mathrm{A} \cap \mathrm{B} \cap \mathrm{C})$

Failure regions: A - fatigue; B - excessive displacement; C - excessive rotation

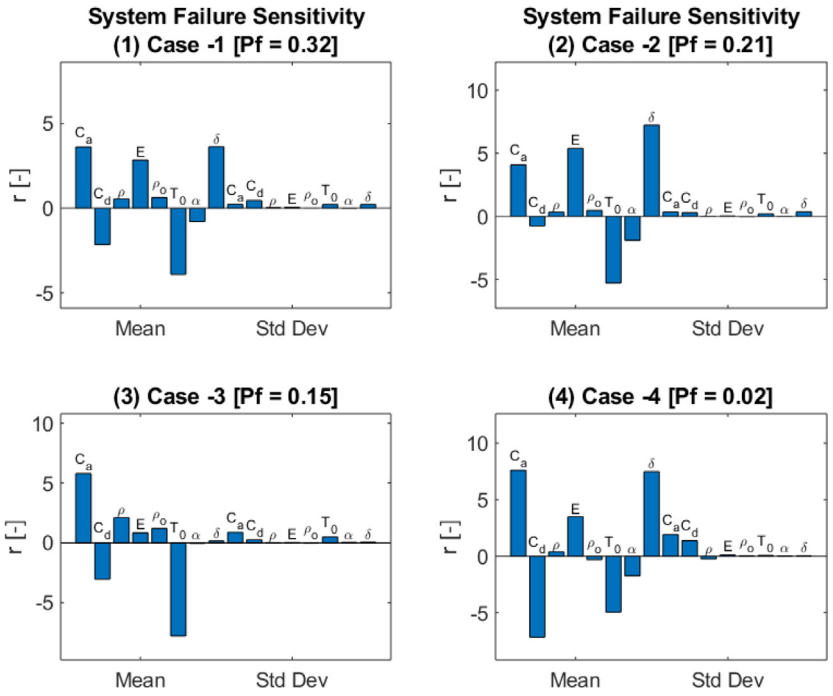

Fig. 5. Sensitivities of system failure probability corresponding to the four cases in Table 2. Same key as Fig. 4.

The system failure probabilities and the corresponding sensitivities for the four cases are shown in Fig. 5. The failure probability for case 1 is the highest because occurrence of any individual failure modes would result in system failure. On the other hand, case 4 has the smallest failure probability because system fails only when all three individual modes of failure happen at the same time. Cases 2 and 3 have similar level of failure probability, however, the dominant variables of the sensitivity vectors are different. The system failure probability in Case 2 is found to be most sensitive to the S–N coefficient δ, while the biggest element of the sensitivity vector for Case 3 is the top tension T_0 and the coefficient δ is insignificant in this case.

The system failure sensitivities of the four different cases are projected onto the singular vectors of the **R** matrix and these are shown in Fig. 6(a). It can be seen from Fig. 6(a) that the projection onto the first singular vector, which has the largest corresponding singular value, is the highest out of the three singular vectors. And this is the same for all four different cases of system failure configurations. In Fig. 6(b), the projection of the sensitivity onto the singular vectors are shown for the three individual failure modes. It can be seen from Fig. 6(b) that both fatigue and excessive rotation failures have higher projection onto the first two singular vectors, while the projection of the failure sensitivity for excessive displacement are higher for the second and third singular vectors. It is therefore clear from Fig. 6 that the vectors that perturb the combined failure probability the most, are the singular vectors with the largest singular values. Further discussions about this are given in Section 4.1. In addition, the usefulness of the sensitivity results would diminish when there are large differences in terms of magnitude between the failure probabilities of individual failure modes and this situation is further discussed in Section 4.3.

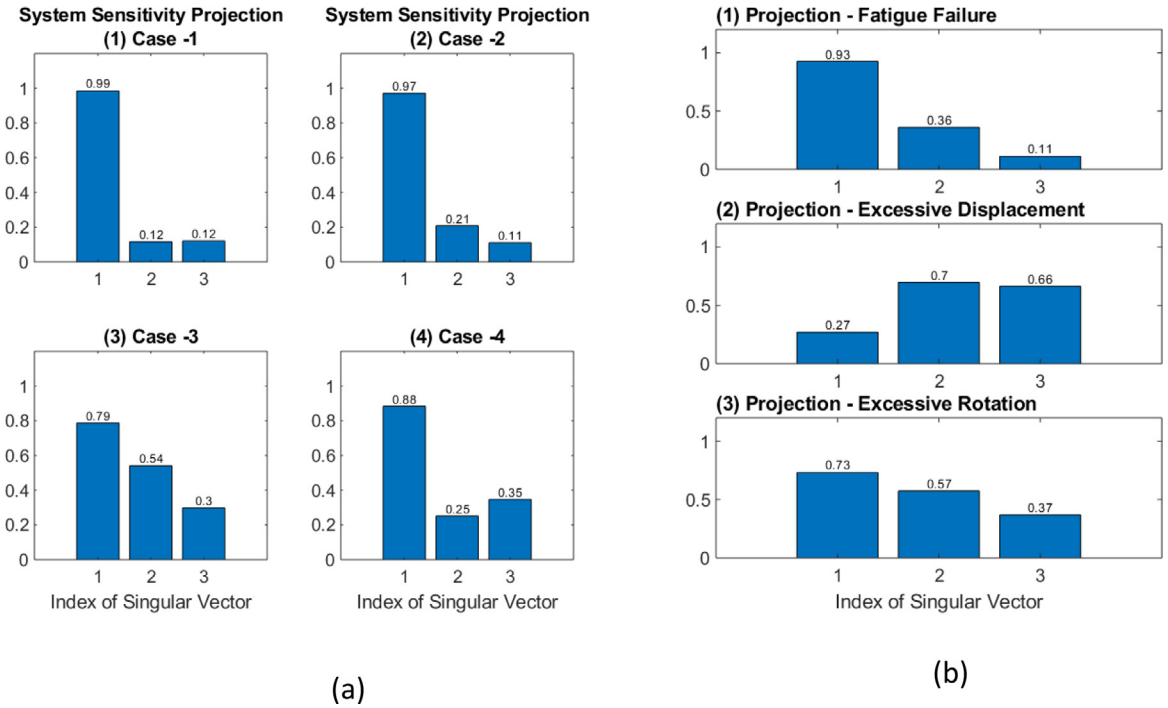

Fig. 6. Projection of sensitivity vectors onto the singular vectors of matrix **R**. The projection values are normalised, where the squared sum of the projections onto the three singular vectors is equal to one. (a) Projection of system failure sensitivities for the four different cases considered in Table 2. (b) Projection of the three individual failure sensitivities.

4. Discussion

4.1. Dominant singular vectors of **R** *give the most sensitive parameters*

The failure sensitivities of the individual modes from the same system are often interdependent. For example, the three individual failure modes of the marine riser studied in Section 3, excessive displacement, excessive rotation and fatigue, might seem to be independent because they are proportional to different orders of derivatives of the displacement, as seen in Appendix B. However, Fig. 6(b) with projections onto the singular vectors of **R** indicate correlations among the sensitivity vectors of individual failure modes. Different failure modes are expected to be correlated in general because they are dependent on the same input parameters for the same system. Therefore, when there are multiple failure modes, it is the combined sensitivity that needs to be addressed. In this case, designers would want to understand that given fixed resources (e.g. time and budget), which uncertain parameters should be focused on to achieve the largest effect on the system failure. A fixed budget often puts a constraint on how much efforts can be spend on reducing parameter uncertainties. Mathematically, that can be translated as a constraint on the norm of the relative change of the parameter vector **b** (denoted as vector $\boldsymbol{\beta}$ in Appendix A). Taking this point of view, as shown in Appendix A, the vector that perturbs the combined failure probability the most, are the singular vectors with the largest singular values. This is evident from the case study of the marine riser in Section 3.4. As shown in Fig. 6(a), in the four cases considered, with different configurations of joint probability of multiple failure modes, it is the first singular vector of matrix **R** that dominates the projection of system failure sensitivities.

4.2. Weighting of failure sensitivity

As discussed in Section 2.3.1, the information about the system sensitivity is related to the linear combinations of the independent individual failure sensitivities. In the case of known joint failure probability, e.g. a specific case in Table 2, the Likelihood Ratio method, implemented using Eqs. (14) and (15), would give the sensitivities for

both individual and system failure probabilities. In this case, we can find the relative weighting of the individual failure modes:

$$\mathbf{Rw} = \mathbf{s} \tag{16}$$

where $\mathbf{w}$ is the weight coefficient vector and $\mathbf{s}$ is the system failure sensitivity vector. The solution to this can be found via pseudoinverse of $\mathbf{R}$

$$\mathbf{w}^{+} = \mathbf{R}^{+}\mathbf{s} \tag{17}$$

and this is practically conducted via singular value decomposition (SVD) of $\mathbf{R}$. Therefore, even if the system failure sensitivity is known, the singular vectors of $\mathbf{R}$ still provide useful information about the relative weighting of individual modes to help targeting the resources for system design improvement.

4.3. Proportional sensitivity

The proportional sensitivity r, as defined in Eq. (4), measures the percentage change on P_{f} resulting from a fraction change of b and it allow us to compare the relative sensitivities of parameters of different physical units because it is unitless. In addition, the formulation of r is the same for different types of distribution parameters and that makes it straightforward to implement. However, two points need to be noted.

First, in practice, proportional change of distribution parameters might be unrealistic. For example, unless the probability distribution of the input variables is far from the real distribution, it is most likely that the change of the mean should be within one standard deviation. From Figs. 4 and 5, we have seen that the sensitivity vectors, for both individual and system failures, are dominated by the mean values of the random variables considered, except for C_{a} and C_{d} when they are significant for failure sensitivities. This is because the coefficients of variation (CoV), as used in the example case study listed in Table 1, are relatively small values. Since proportional sensitivity r is used, small values of CoV limit the range of variation for the standard deviation value. Considering the practical implications of the mean and standard deviation, it makes sense to consider instead a relative sensitivity, between mean and standard deviation of the same variable, to be normalised by the standard deviation. In the case of Gaussian distribution with parameters of mean (μ) and standard deviation (σ), instead of r_{jk} in Eq. (4), the sensitivity that is normalised by standard deviation is given by:

$$\hat{r}_{jk} = \frac{\partial P_{\mathrm{f}}^{(k)}}{\partial \mu_j}\frac{\sigma_j}{P_{\mathrm{f}}^{(k)}} = \frac{\partial P_{\mathrm{f}}^{(k)}}{\partial \mu_j}\frac{\mu_j}{P_{\mathrm{f}}^{(k)}}\frac{\sigma_j}{\mu_j} = r_{jk}\frac{\sigma_j}{\mu_j} \tag{18}$$

where the modified sensitivity index is obtained multiplying the original proportional sensitivity by the CoV. As pointed out in [26], the use of the standard deviation as a scale factor implies the allowable design range of the mean value is limited to local region and it is quantified by the standard deviation. In case there is a specific requirement to make big changes to the mean value, the random variable should be treated as a design variable for the analysis.

Second, the absolute values of proportional sensitivity r tend to be higher for small probability of failure. This is not an issue for sensitivity of individual failure modes because the relative ratios are unaffected among the parameters. However, the first singular vector of sensitivity matrix $\mathbf{R}$ tends to be dominated by the failure modes with low failure probability. This would lead us to focus our resources on the failure modes that are unlikely to occur. Nevertheless, in the situation with one dominant failure mode, it is most likely that the sensitivity information of the individual failure modes are sufficient to target that specific mode. When the failure probability of the dominant mode is reduced and the failure probabilities of different failure modes become comparable, the combined sensitivity analysis proposed in Section 2.3.2 can then be used to make informed decisions.

4.4. Random threshold

In this paper, fixed failure thresholds are assumed for the failure modes. If we are uncertain about the threshold z but it can be specified by a PDF $p(z)$, then following Eq. (4) the expected proportional sensitivity can be computed as:

$$\mathbb{E}\left[r_{jk}\right] = \int \frac{\partial P_{\mathrm{f}}^{(k)}(z)}{\partial b_j}\frac{b_j}{P_{\mathrm{f}}^{(k)}(z)}p(z)\,\mathrm{d}z \tag{19}$$

For system failure analysis, the sensitivity matrix can be assembled in the same way as Eq (11), but in this case we compute singular vectors for the expected sensitivity matrix $\mathbb{E}[\mathbf{R}]$ for combined sensitivities.

5. Conclusions

Sensitivity analysis is of fundamental importance for design in the presence of uncertainties. In this paper, a sensitivity matrix $\mathbf{R}$ has been proposed to study the relative importance of random parameters for system failure probabilities with multiple failure modes. The set of parameters that perturbs the combined failure probability the most are found to be given by the singular vectors of $\mathbf{R}$ with largest singular values. This indicates that for system failure sensitivity, as demonstrated by the case study, we can extract most information from the dominant singular vectors. As a result, the sensitivity matrix $\mathbf{R}$ can provide information to guide designers to focus resources on reducing uncertainties of the most sensitive parameters, not just for individual failure modes but also for system failure probabilities and it is especially useful when the system configuration of the failure modes are unknown.

It has been demonstrated in this paper that the combination of Monte Carlo and Likelihood Ratio methods provides an efficient one-run simulation to obtain the unconditional failure probability and its first derivatives. Taking the mathematical expectation perspective of the unconditional failure probability, one of the future research is to look at forming $\mathbf{R}$ matrix for different probabilistic performance measures. In addition, to have wider applications, advanced Monte Carlo methods are needed for efficient simulation of large number of samples and it would be necessary to incorporate deterministic variables in the sensitivity analysis for design optimisations.

Declaration of competing interest

The authors declare that they have no known competing financial interests or personal relationships that could have appeared to influence the work reported in this paper.

Acknowledgment

This work has been funded by the Engineering and Physical Sciences Research Council, UK through the award of a Programme Grant “Digital Twins for Improved Dynamic Design”, Grant No. EP/R006768.

Appendix A. Constrained optimisation for combined sensitivity

For multiple failure modes, we can look at the combined perturbation:

$$\Omega = \sum_k \left(\frac{\Delta P_{\mathrm{f}}^{(k)}}{P_{\mathrm{f}}^{(k)}} \right)^2 \tag{A.1}$$

The first order perturbed failure probability for each mode is:

$$\Delta P_{\mathrm{f}}^{(k)} = \sum_j \Delta b_j \frac{\partial P_{\mathrm{f}}^{(k)}}{\partial b_j} = P_{\mathrm{f}}^{(k)} \sum_j r_{jk} \frac{\Delta b_j}{b_j} \tag{A.2}$$

where r_{jk} is defined in Eq. (4). Substituting Eq. (A.2) into Eq. (A.1), we get:

$$\begin{aligned} \Omega &= \sum_k^m \left(\sum_i^n r_{ik} \frac{\Delta b_i}{b_i} \right) \left(\sum_j^n r_{jk} \frac{\Delta b_j}{b_j} \right) \\ &= \sum_i \sum_j \beta_i \beta_j \left(\sum_k r_{ik} r_{jk} \right) n \\ &= \boldsymbol{\beta}^{\mathrm{T}} \mathbf{R} \mathbf{R}^{\mathrm{T}} \boldsymbol{\beta} \end{aligned} \tag{A.3}$$

where $\mathbf{R}$ is the sensitivity matrix given in Eq. (11) and the ith element in vector $\boldsymbol{\beta}$ is $\beta_i = \Delta b_i / b_i$. To maximise

the combined perturbation, the method of Lagrange Multiplier can be used to solve the constrained optimisation:

$$L = \frac{1}{2}\boldsymbol{\beta}^{\mathrm{T}}\mathbf{R}\mathbf{R}^{\mathrm{T}}\boldsymbol{\beta} - \lambda(\boldsymbol{\beta}^{\mathrm{T}}\boldsymbol{\beta} - \epsilon) \tag{A.4}$$

$$\frac{\partial L}{\partial \boldsymbol{\beta}} = \mathbf{R}\mathbf{R}^{\mathrm{T}}\boldsymbol{\beta} - \lambda\boldsymbol{\beta} = \mathbf{0} \tag{A.5}$$

where λ is the Lagrange multiplier. Eq. (A.5) is equivalent to the following eigenvalue problem:

$$\mathbf{R}\mathbf{R}^{\mathrm{T}}\boldsymbol{\beta} = \lambda\boldsymbol{\beta} \tag{A.6}$$

and the vector that perturbs the combined failure probability the most, is the eigenvector with the largest eigenvalue. In practice, it is more efficient to solve for the singular vectors of $\mathbf{R}$, and the singular values of $\mathbf{R}$ are square roots of the corresponding eigenvalues of $\mathbf{R}\mathbf{R}^{\mathrm{T}}$.

Appendix B. Dynamic model of the marine riser

A top-tensioned TLP marine riser is a fluid conduit that between subsea equipment and a surface platform. Its primary function is to convey fluids to and from the floating platform. The dynamic model of the marine riser used here is based on [23] and only the quantities related to this paper are briefly introduced below. As shown in Fig. 2, both ends of the riser are ball jointed and there is a prescribed top motion. The Rayleigh–Ritz method is used to approximate the structure displacement response with a finite expansion:

$$v(x,\omega) = \sum_{m=1}^{n} \varphi_m(x) q_m(\omega) \tag{B.1}$$

where x is the coordinate along the riser from the mean water level as indicated in Fig. 2. φ is the shape function and q is the generalised coordinate. The other quantities of interest in this paper are the small rotation:

$$\theta\,(x,\omega) = \frac{\partial v\,(x,\omega)}{\partial x} \tag{B.2}$$

and the bending stress:

$$\beta\,(x,\omega) = \frac{1}{2} E D_{\mathrm{o}} \frac{\partial^2 v\,(x,\omega)}{\partial x^2} \tag{B.3}$$

where E is the Young's modulus and D_{o} is the outer diameter of the marine riser.

For a random wave excitation, the quantity of interest is the spectral density of the response. Assuming a stationary random process, the root mean square (r.m.s.) value is related to the one sided spectral density $S_v(x,\omega)$ as:

$$\sigma_v^2(x) = \sum_{\omega} 2 S_v(x,\omega) d\omega \tag{B.4}$$

and the r.m.s. value for the rotation and bending stress responses can be obtained in the same way.

The fluid forces in frequency domain are modelled using the semi-empirical Morison's equation [27]:

$$F(x,\omega) = \left[-\omega^2 \rho_{\mathrm{f}} A\,(x)\,(1 + C_{\mathrm{a}}) + \frac{1}{2} i\omega C_{\mathrm{d}} \gamma\,(x)\,\rho_{\mathrm{f}} D\,(x)\right] a_{\mathrm{w}} e^{-k_{\mathrm{w}} x} \tag{B.5}$$

where C_{a} and C_{d} are the inertia and drag coefficients. A and D are the cross-section area and the diameter. ρ_{f} is the water density, a_{w} is the wave amplitude and k_{w} is the wave number. Since drag force is dependent on the relative velocity squared, in frequency domain, a linearisation coefficient γ [28] is introduced:

$$|u_{\mathrm{r}}|\,u_{\mathrm{r}} = |u - \dot{v}|\,(u - \dot{v}) \approx \gamma\,(u - \dot{v}) \tag{B.6}$$

where u_r is the relative velocity. And for random wave, this linearisation coefficient is [28]

$$\gamma(x) = \sqrt{\frac{8}{\pi}}\sigma_{\mathrm{u_r}}(x) \tag{B.7}$$

where σ_{u_r} is r.m.s. value for the relative velocity at each position along the riser. Since the linearisation coefficient γ is dependent on the velocity response of the riser, the fluid forces in Eq. (B.5) are computed iteratively with the γ updated at each iteration based on the computed riser response.

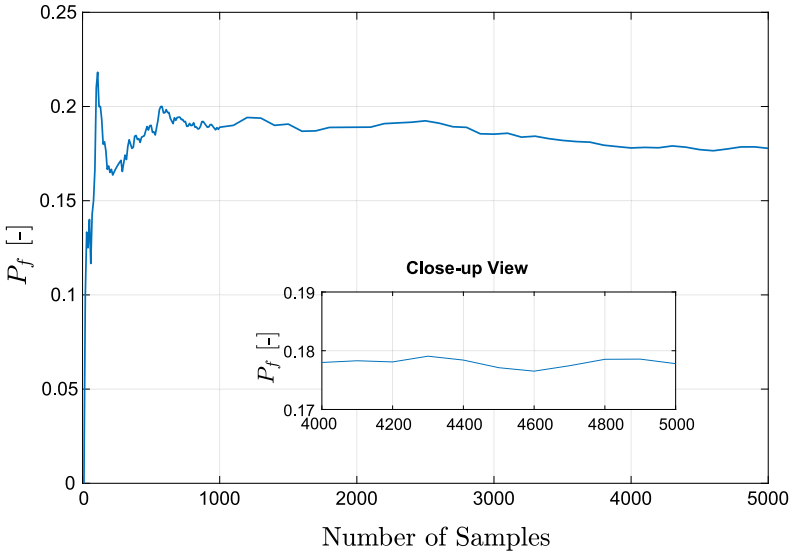

Fig. C.1. Convergence of the unconditional probability of fatigue failure as a function of number of samples used in the Monte Carlo simulation. The close-up view shows the magnified range between 4000 and 5000 samples.

Appendix C. Convergence and validation analysis

In this section, the convergence and validation analysis is conducted using the fatigue failure mode as an example. The parameters used in this section are the same as Section 3 where the fatigue life threshold of 80 years is used (for the perturbation validation analysis in Fig. C.3, a range of thresholds is computed for a more comprehensive comparison).

Fig. C.1 shows the unconditional fatigue failure probability P_{f} as a function of the number of samples considered in the Monte Carlo simulation (c.f. Algorithm 1 in Section 2.5). Fig. C.2 presents the sensitivity factors r_{μ} (sensitivity to the mean) and r_{σ} (sensitivity to the standard deviation) related to each one of the uncertain parameters as a function of the number of samples. A good convergence is observed for both failure probability and the sensitivities.

The convergence tests performed in Figs. C.1 and C.2 assess the accuracy of the Monte Carlo simulation. To validate the proposed sensitivity estimation using the Likelihood Ratio method, Fig. C.3 presents a comparison between the exact and approximate perturbation of the probability of failure, where each one of the uncertain parameters (b_j) is perturbed by 5%. Only the perturbation of the mean values (μ) of the uncertain variables are shown in the figure because their standard deviations have negligible influence on the failure probability for the case considered here as seen in Fig. 4. The exact method calculates the change of the failure probability by $\Delta P_{\mathrm{f}}^{j} = P_{\mathrm{f}}\left(\mathbf{b} + \Delta b_j\right) - P_{\mathrm{f}}(\mathbf{b})$ with direct perturbation of the input parameters. In comparison, the approximation calculates the perturbation via 1st order perturbation $\Delta P_{\mathrm{f}}^{j} = \Delta b_j \partial P_{\mathrm{f}}/\partial b_j$. To have a more comprehensive comparison, the results in Fig. C.3 are calculated for a range of failure threshold between 60 and 100 years of service life (the case study in Section 3 uses 80 years as the threshold for the fatigue failure).

The results presented in Fig. C.3, computed using 2500 samples, show a reasonable agreement between the exact and the approximate ΔP_{f}. As the approximate method is a 1st order approximation, the observed differences in Fig. C.3 maybe due to the contribution of the omitted higher order terms in the Taylor expansion of ΔP_{f}. This is evident from Fig. C.3 that the biggest deviation is for the S–N parameter δ where the total damage received by the structure depends on a factor raised to the δ power.

In terms of computational cost, the exact results are based on perturbing one parameter at a time, for example, the calculation shown in Fig. C.3 had to be repeated 8 times for the 8 parameters to get the exact results. The computational cost will inevitably become prohibitive as the number of parameters gets larger. On the other hand, the proposed method using the Likelihood Ratio method just requires a single run to get the sensitivities to all parameters of interest. Although the sensitivity is based on 1st order approximation of the perturbation, the validation

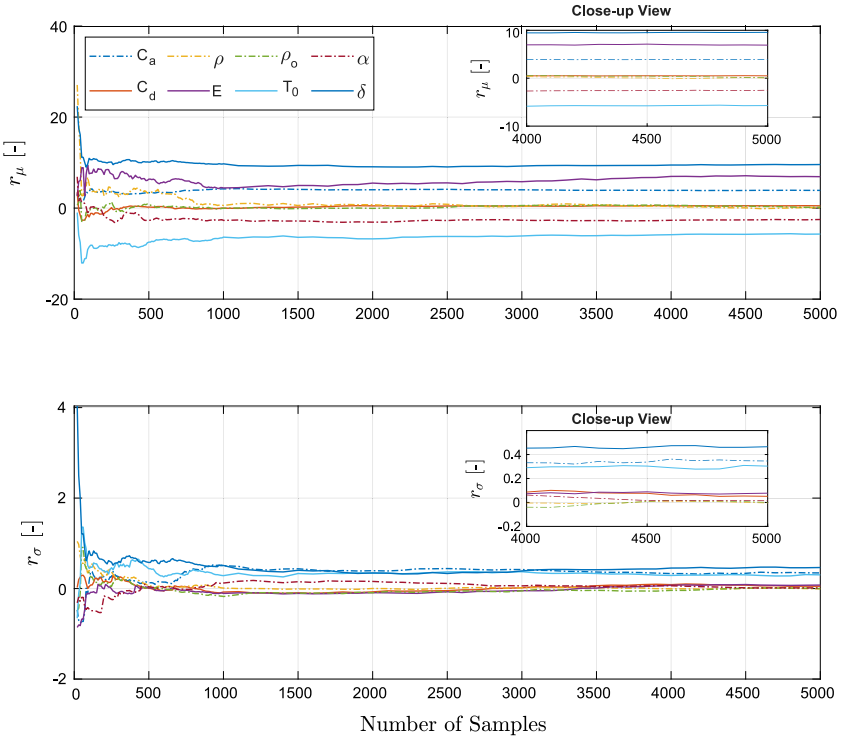

Fig. C.2. Convergence of the proportional sensitivity for the probability of fatigue failure as a function of number of samples used in the Monte Carlo simulation. The close-up view shows the magnified range between 4000 and 5000 samples. Top figure shows the sensitivity to the mean of the random variables; Bottom figure for the sensitivity to the standard deviation.

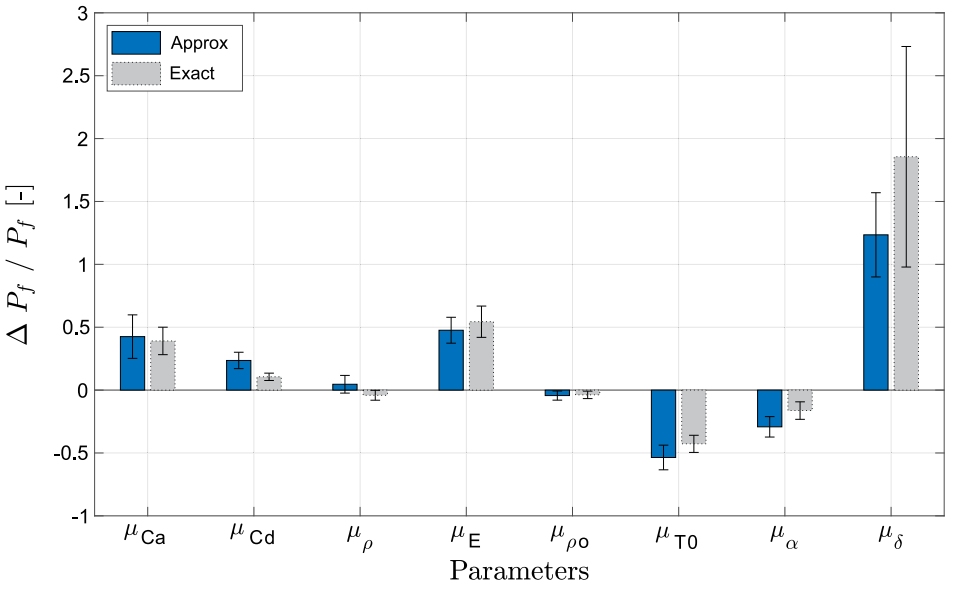

Fig. C.3. Perturbation results of the fatigue failure probability using two different approaches. The 'Exact' method calculates the perturbation by $\Delta P_{\mathrm{f}}^{j} = P_{\mathrm{f}}\left(\mathbf{b} + \Delta b_j\right) - P_{\mathrm{f}}(\mathbf{b})$. The 'Approx' method is based on a 1st order approximation $\Delta P_{\mathrm{f}}^{j} = \Delta b_j \partial P_{\mathrm{f}} / \partial b_j$. The results are calculated for a range of fatigue failure thresholds between 60 and 100 years of service life. The bars indicate the averaged value across different failure thresholds, with the standard deviation given by the error bars.

results demonstrate that designers can use the proposed method to identify the influential parameters and potentially conduct more focused analysis to improve the design.

References

[1] J.C. Helton, J.D. Johnson, W.L. Oberkampf, An exploration of alternative approaches to the representation of uncertainty in model predictions, Reliab. Eng. Syst. Saf. 85 (2004) 39–71, http://dx.doi.org/10.1016/j.ress.2004.03.025.

[2] A. Keane, P. Nair, Computational Approaches for Aerospace Design: The Pursuit of Excellence, Wiley, 2005.

[3] N. Lelièvre, P. Beaurepaire, C. Mattrand, N. Gayton, A. Otsmane, On the consideration of uncertainty in design: optimization - reliability - robustness, Struct. Multidiscip. Optim. 54 (2016) 1423–1437, http://dx.doi.org/10.1007/s00158-016-1556-5.

[4] M.A. Valdebenito, G.I. Schuëller, A survey on approaches for reliability-based optimization, Struct. Multidiscip. Optim. 42 (2010) 645–663, http://dx.doi.org/10.1007/s00158-010-0518-6.

[5] H.-G. Beyer, B. Sendhoff, Robust optimization – A comprehensive survey, Comput. Methods Appl. Mech. Engrg. 196 (2007) 3190–3218, http://dx.doi.org/10.1016/j.cma.2007.03.003.

[6] A. Saltelli (Ed.), Global Sensitivity Analysis: The Primer, John Wiley, Chichester, England ; Hoboken, NJ, 2008.

[7] H.A. Jensen, M.A. Valdebenito, G.I. Schuëller, D.S. Kusanovic, Reliability-based optimization of stochastic systems using line search, Comput. Methods Appl. Mech. Engrg. 198 (2009) 3915–3924, http://dx.doi.org/10.1016/j.cma.2009.08.016.

[8] L. Wang, Y. Liu, D. Liu, Z. Wu, A novel dynamic reliability-based topology optimization (DRBTO) framework for continuum structures via interval-process collocation and the first-passage theories, Comput. Methods Appl. Mech. Engrg. 386 (2021) 114107, http://dx.doi.org/10.1016/j.cma.2021.114107.

[9] M.S. Eldred, H.C. Elman, Design under uncertainty employing stochastic expansion methods, Int. J. Uncertain. Quantif. 1 (2011) http://dx.doi.org/10.1615/Int.J.UncertaintyQuantification.v1.i2.20.

[10] V. Keshavarzzadeh, H. Meidani, D.A. Tortorelli, Gradient based design optimization under uncertainty via stochastic expansion methods, Comput. Methods Appl. Mech. Engrg. 306 (2016) 47–76, http://dx.doi.org/10.1016/j.cma.2016.03.046.

[11] J.O. Royset, E. Polak, Reliability-based optimal design using sample average approximations, Probab. Eng. Mech. 19 (2004) 331–343, http://dx.doi.org/10.1016/j.probengmech.2004.03.001.

[12] M.A. Valdebenito, G.I. Schuëller, Efficient strategies for reliability-based optimization involving non-linear, dynamical structures, Comput. Struct. 89 (2011) 1797–1811, http://dx.doi.org/10.1016/j.compstruc.2010.10.014.

[13] Z. Wang, R. Ghanem, An extended polynomial chaos expansion for PDF characterization and variation with aleatory and epistemic uncertainties, Comput. Methods Appl. Mech. Engrg. 382 (2021) 113854, http://dx.doi.org/10.1016/j.cma.2021.113854.

[14] J.C. Spall, Introduction to Stochastic Search and Optimization: Estimation, Simulation, and Control, Wiley-Interscience, Hoboken, N.J, 2003.

[15] C. Proppe, Local reliability based sensitivity analysis with the moving particles method, Reliab. Eng. Syst. Saf. 207 (2021) 107269, http://dx.doi.org/10.1016/j.ress.2020.107269.

[16] J. He, X. Guan, Uncertainty sensitivity analysis for reliability problems with parametric distributions, IEEE Trans. Reliab. 66 (2017) 712–721, http://dx.doi.org/10.1109/TR.2017.2714172.

[17] H.A. Jensen, F. Mayorga, M.A. Valdebenito, Reliability sensitivity estimation of nonlinear structural systems under stochastic excitation: A simulation-based approach, Comput. Methods Appl. Mech. Engrg. 289 (2015) 1–23, http://dx.doi.org/10.1016/j.cma.2015.01.012.

[18] J. Li, A. Mosleh, R. Kang, Likelihood ratio gradient estimation for dynamic reliability applications, Reliab. Eng. Syst. Saf. 96 (2011) 1667–1679, http://dx.doi.org/10.1016/j.ress.2011.08.001.

[19] W.A. Link, P.F. Doherty, Scaling in sensitivity analysis, Ecology 83 (2002) 3299–3305, http://dx.doi.org/10.2307/3072080.

[20] J. Kirch, C. Thomaseth, A. Jensch, N.E. Radde, The effect of model rescaling and normalization on sensitivity analysis on an example of a MAPK pathway model, EPJ Nonlinear Biomed. Phys. 4 (2016) 3, http://dx.doi.org/10.1140/epjnbp/s40366-016-0030-z.

[21] B.J. Bichon, J.M. McFarland, S. Mahadevan, Efficient surrogate models for reliability analysis of systems with multiple failure modes, Reliab. Eng. Syst. Saf. 96 (2011) 1386–1395, http://dx.doi.org/10.1016/j.ress.2011.05.008.

[22] G. Stavroulakis, D.G. Giovanis, M. Papadrakakis, V. Papadopoulos, A new perspective on the solution of uncertainty quantification and reliability analysis of large-scale problems, Comput. Methods Appl. Mech. Engrg. 276 (2014) 627–658, http://dx.doi.org/10.1016/j.cma.2014.03.009.

[23] C.L. Kirk, Dynamic response of marine risers by single wave and spectral analysis methods, Appl. Ocean Res. 7 (1985) 2–13, http://dx.doi.org/10.1016/0141-1187(85)90013-6.

[24] Subrata K. Chakrabarti, in: Subrata K. Chakrabarti (Ed.), Handbook of Offshore Engineering, first ed., Elsevier, London, 2005.

[25] Det Norske Veritas (DNV), Recommended Practice DNV-RP-F204-Riser Fatigue, Hovik, Norway, 2010.

[26] Y.-T. Wu, Computational methods for efficient structural reliability and reliability sensitivity analysis, AIAA J. 32 (1994) 1717–1723, http://dx.doi.org/10.2514/3.12164.

[27] T. Sarpkaya, Mechanics of Wave Forces on Offshore Structures, Van Nostrand Reinhold, New York, 1981.

[28] Y.M. Low, R.S. Langley, Time and frequency domain coupled analysis of deepwater floating production systems, Appl. Ocean Res. 28 (2006) 371–385, http://dx.doi.org/10.1016/j.apor.2007.05.002.